International Journal of Engineering and Science Applications
ISSN 2406-9833

IJEScA

Robust Control of Hydro-Thermal Power System Considering Energy Capacitor System

Thongchart Kerdphol, Yaser Qudaih, and Yasunori Mitani
Department of Electrical and Electronic Engineering, Kyushu Institute of Technology
1-1 Sensui-cho, Tobata-ku, Kitakyushu-shi,
Fukuoka, 804-8550, Japan.
n589504k@mail.kyutech.jp, yaser_qudaih@yahoo.com, mitani@ele.kyutech.ac.jp

ABSTRACT

This article proposes a robust controller design of hydro-thermal power system considering of the thermal power plant area connected to the hydro power plant area. The automation generation control of an interconnected hydro-thermal power system with a small Energy Capacitor System (ECS) augmented to both area has been investigated. The controller is used in order to control the frequency robustly and to improve the power system stability due to the uncertainties in load change and energy capacitors in the system. The power from the load changes are introduced into the system and treated it as the uncertainty during the design process. The H-infinity loop-shaping design procedure (H-infinity LSDP) is adopted as the control design procedure in this study. The results reveal that H-infinity LSDP can achieve higher performance and more robustness compared with PID controller.

Keywords: Energy Capacitor System, H-infinity LSDP, Power system Oscillation, Robust Control
Article history: Received 06 October 2014, last received in revised 18 November 2014

1. INTRODUCTION

Nowadays, an energy storage device with a fast response time can be installed to power system in order to decrease the frequency oscillations of the system usually occurred due to random load scheme. Various energy storage devices have been designed and presented in the previous decades such as batteries, compressed air storage, flywheels, fuel cells, hydro pumped storage, Energy Capacitor System (ECS), Super Magnetic Energy Storage (SMES) and so on [1]-[3]. ECS is one of the latest in energy storage devices. There are many advantage of ECS such as fast response, free maintenance, long life and environmental friendly [4]-[6]. This paper investigated the dynamics performance of both PID and H_∞ -LSDP controller and take the advantage of ECS in an interconnected hydro-thermal power plant to improve the system stability.

In the previous decades, the two area power system has been considered as research targets such as thermal - thermal area or hydro – thermal area. In which one of the area is hydro and other will be thermal or hydro. They are interconnected via tie line. In order to control the system frequency, the speed governor which acts as the primary controller matches the supply with the demand. Moreover, the secondary controller tunes the frequency and tie line power [7-9].

This paper proposes the H_∞ -LSDP controller design of hydro – thermal power

system considering ECS with the addition of wind power source and treating it as the disturbance to the power system. The method is based on H_∞-LSDP with the main purpose of decreasing the oscillations of frequency after installing ECS and wind power sources to the power system [10] and [11]. For the performance verification, the PID controller configuration is selected to be the candidate for comparison against the former and their parameters are optimally tuned by Genetic Algorithm (GA) [12] in order to compare the dynamic stability in the hydro – thermal power system [13]. The results reveal that H_∞-LSDP can achieve higher performance and more robustness compared with conventional PID controller of which the parameters tuned by GA. In addition, the efficient usage of the ECS was clearly illustrated and approved.

2. DYNAMIC MODEL OF INTERCONNECTED HYDRO – THERMAL POWER SYSTEM WITH THE ECS SYSTEM.

The hydro – thermal power system is shown in Figure 1. In both of the two areas energy capacitor system (ECS) are installed. Each area would be subjected to load variation. Two areas are connected via tie line in order to transfer power between areas and enhance system stability.

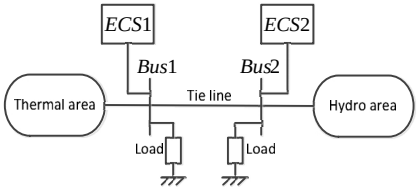

Figure 1. The hydro-thermal power system incorporating the ECS

The thermal area comprises the speed governor acting as a primary controller. It supports to meet the generation with the demand by regulating the steam input to the turbine. The reference power setting of the governor is changed by the secondary controller so as to tune the system frequency.

A. The Thermal Area Formulation.

The speed governor equation :

$$\Delta P_{G_1} = \Delta P_{ref_1} - \frac{1}{R_1}\Delta f_1 \tag{1}$$

The hydraulic amplifier equation is:

$$\Delta P_{H_1} = \left(\frac{1}{1+sT_G}\right)\Delta P_{G_1} \tag{2}$$

The non-reheat turbine equation is:

$$\Delta P_{T_1} = \left(\frac{1}{1+sT_T}\right)\Delta P_{H_1} \tag{3}$$

B. The Hydro Area Formulation.

The speed governor equation is:

$$\Delta P_{G_2} = \Delta P_{ref_2} - \frac{1}{R_2}\Delta f_2 \tag{4}$$

$$\Delta P_{Hg} = \left(\frac{1}{1+sT_1}\right)\Delta P_{G_2} \tag{5}$$

$$\Delta P_{H_2} = \left(\frac{1+sT_R}{1+sT_2}\right)\Delta P_{Hg} \tag{6}$$

The hydro turbine equation is:

$$\Delta P_{T_2} = \Delta P_{H_2}\left(\frac{1-sT_W}{1+0.5sT_W}\right) \tag{7}$$

The power output from turbine becomes an input to the generator in order to feed

electrical power to the system. This equation can be shown as:

$$\Delta P_{T_i} - \left(\Delta P_{D_i} + \Delta P_{ECS_i}\right) = \Delta f_i \left(\frac{K_{P\ i}}{1 + sT_{P\ i}} \right) \quad (8)$$

where i = 1, 2

The power transfer equation between two area via tie line and is expressed as:

$$\Delta P_{tie} = \frac{2\textcircled{R}T_{12}}{s}\left(\Delta f_1 - \Delta f_2\right) \quad (9)$$

Because of load deviation, each area faces the frequency deviation apart from tie line power deviation. This problem can solved by using the Area Control Error (ACE). This equation followed in this paper is shown as:

$$\Delta ACE_i = \Delta P_{tie,i} + {}_i\Delta f_i \quad (10)$$

where i = 1, 2

C. The Energy Capacitor System.

A energy capacitor system collects the energy in its electrostatic field created at its plates in response to resolved potential across it. Figure 2 shows the general structure of the ECS system.

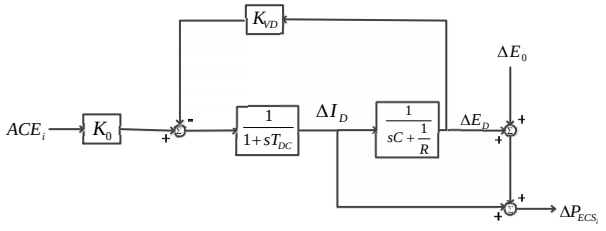

Figure 2. The ECS model structure.

The ACE is fed as control signal to the ECS unit. The relative equation between AEC to ECS unit can be expressed as:

$$\Delta I_{D_i} = \left(\frac{1}{1 + sT_{dc}} \right)\left(K_{ECS}\Delta ACE_i - K_{VD}\,\Delta E_{D_i}\right) \quad (11)$$

where i = 1, 2

The power output from the ECS unit is shown as:

$$\Delta P_{ECS_i} = \Delta I_{D_i}\left(E_{D_0} + \Delta E_{D_i}\right) \quad (12)$$

Where

$$\Delta E_{D_{1,2}} = \frac{\Delta I_{D_{1,2}}}{C + \frac{1}{R}} \quad (13)$$

Where

$\Delta P_{G_1}, \Delta P_{G_2}$ are the governor power deviation of the thermal and hydro power plant respectively.

$\Delta P_{ref_1}, \Delta P_{ref_2}$ are the reference power deviation of the thermal and hydro power plant respectively.

$\Delta f_1, \Delta f_2$ are the frequency deviation of the thermal and hydro power plant respectively.

$_1$, $_2$ are the frequency bias constant in the thermal and hydro power plant respectively.

R_1, R_2 are the regulation of speed governor constant in the thermal and hydro power plant respectively.

$\Delta P_{H_1}, \Delta P_{H_2}$ are the hydraulic value power deviation of the thermal and hydro power plant respectively.

$\Delta P_{T_1}, \Delta P_{T_2}$ are the turbine power deviation of the thermal and hydro power plant respectively.

ΔP_{Hg} is the hydro governor power deviation of the hydro power plant respectively.

$\Delta P_{ECS_1}, \Delta P_{ECS_2}$ are the ECS power deviation of the thermal and hydro power plant respectively.

ΔP_{tie} is the tie line power deviation.

$\Delta P_{D_1}, \Delta P_{D_2}$ are the load power deviation of the thermal and hydro power plant respectively.

$\Delta ACE_1, \Delta ACE_2$ are the automatic control error deviation of the thermal and hydro power plant respectively.

$\Delta I_{D_1}, \Delta I_{D_2}$ are the current deviation of the ECS in the thermal and hydro power plant respectively.

$\Delta I_{D_1}, \Delta I_{D_2}$ are the current deviation of the ECS in the thermal and hydro power plant respectively.

$\Delta E_{D_1}, \Delta E_{D_2}$ are the voltage deviation of the ECS in the thermal and hydro power plant respectively.

T_G is the governor time constant of the thermal power plant.

T_T is the non-reheat turbine time constant of the thermal power plant.

T_1, T_2, T_R are the time constant of the hydro governor.

T_W is the time constant of the hydro turbine.

T is the synchronizing coefficient.

T_{dc} is the DC voltage time constant of the ECS unit.

T_{P_1}, T_{P_2} are the power system time constant of the thermal and hydro power plant respectively.

K_{P_1}, K_{P_2} are the power system gain of the thermal and hydro power plant respectively.

K_{ECS} is the ECS gain of the thermal and hydro power plant.

K_{VD} is the voltage deviation gain of the ECS in the thermal and hydro power plant.

C is the capacitor of the ECS.

R is the resistance of the ECS.

Linearizing (1)-(13), the resulting state space equations can be expressed as:

$$\dot{X} = AX + BU + CP \quad (14)$$

Where X, U and P are:

$$X = \left[\Delta f_1 \quad \Delta P_{H_1} \quad \Delta P_{T_1} \quad \Delta f_2 \quad \Delta P_{Hg} \quad \Delta P_{H_2} \quad \Delta P_{T_2} \quad \Delta P_{tie} \quad \Delta I_D \quad \Delta E_D \right]^T$$

$$U = \left[\Delta P_{ref_1} \quad \Delta P_{ref_2} \right]^T$$

$$P = \left[\Delta P_{D_1} \quad \Delta P_{D_2} \right]^T$$

The modified hydro-thermal model including the ECS and wind power sources is linear and can be shown in Figure 3. The value of constants are shown in the appendix.

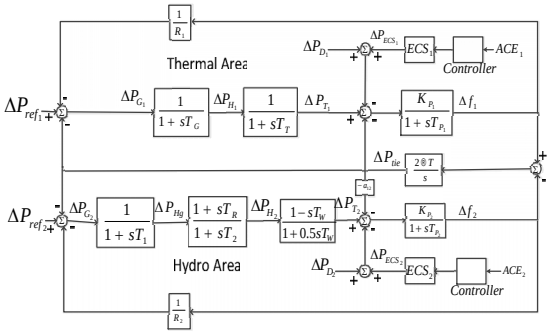

Figure 3. The modified hydro-thermal model including the ECS.

3. THE PROPOSED CONTROL METHOD

A. The Robust Controller Design by H_∞-LSDP.

Figure 4 shows two weighting functions W_1 (for lead compensation) and W_2 (for lag compensation). Then, $G_S = W_2 G W_1$.

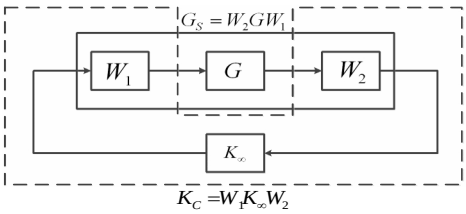

Figure 4. The plant G_S and the robust controller design.

The robust stability can be designed from $K_C = W_1 K_\infty W_2$ where K_∞ is the H_∞ transfer function. The weighting functions, which are W_1 and W_2. In this study, W_2 is selected to be 1.

The H_∞ robust stability starts from shaping plant G_S by factoring the left co-prime of the nominal plant $G_S = \Delta_M^{-1}\Delta_N$ when the plant is disturbed.

$$G_p = \left\{ (M_l + \Delta_M)^{-1}(N_l + \Delta_N) : \left\| \Delta_N \quad \Delta_M \right\|_\infty \le 1/¥ \right\} \quad (15)$$

Where Δ_M and Δ_N are the uncertainty transfer function in the nominal plant G.

From the stability definition of H_∞, G_p and K_C can be synthesized as in Fig. 3. The objective of the robust controller design, not only provide stability to the plant G, but also provide stability to G_p by $1/¥$ in (15) which is the robust stability index.

The robust stability margin of the power system with uncertainty is specified by the minimum value of ¥, that is $¥_{\min}$. According to (16), $¥_{\min}$ can be calculated as follows:

$$¥_{\min} = \sqrt{1 + a_{\max}(XZ)} \quad (16)$$

Where $a_{\max}(XZ)$ is the maximum value of XZ.

The robust controller gain can be designed from (17).

$$K_\infty = \begin{bmatrix} A + BF + ¥^2 (L^T)^{-1} Z C^T (C + DF) & ¥^2 (L^T)^{-1} Z C^T \\ B^T X & -D^T \end{bmatrix} \quad (17)$$

Where $F = -S^{-1}(D^T C + B^T X)$ and $L = (1 - ¥^2) I + XZ$.

Then, determine the value of $K_C(s) = W_1 K_\infty W_2$, according to the constraint in (18).

$$\left\| \begin{bmatrix} I \\ K_\infty \end{bmatrix} (I - G_S K_\infty)^{-1} \begin{bmatrix} I & G_S \end{bmatrix} \right\|_\infty \le ¥ \quad (18)$$

B. The PID Controller with Parameters Optimally Tuned by GA.

Using GA in the tuning procedure to find the suitable parameters K_P, K_I and K_D. The input of controller are AEC_1, AEC_2 and the output of controller are $\Delta P_{ref_1}, \Delta P_{ref_2}$.

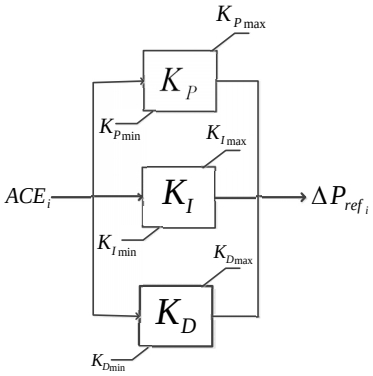

Figure 5. The structure of the supplementary PID controller.

With the cost function of the form:

$$\text{Minimize } J = \int_0^t \left(\Delta f_1^2 + \Delta f_2^2 + \Delta P_{tie}^2\right) \cdot tdt \quad (19)$$

Under the constraints of:

$$K_{P_{\min}} \le K_P \le K_{P_{\max}} \quad ,$$
$$K_{I_{\min}} \le K_I \le K_{I_{\max}}, K_{D_{\min}} \le K_D \le K_{D_{\max}}$$

Where K_P , K_I and K_D correspond to the PID controller gains of the thermal and hydro power plant.

4. SIMULATION RESULTS

In order to demonstrate the efficiency of the proposed method, this paper makes the comparison between the hydro-thermal power system without the ECS and another one equipped the ECS with H_∞ -LSDP. Moreover, the performance verification is done against the PID controller of which parameters tuned by GA.

The value of K_∞ of ΔP_{ref_1} by H_∞ -LSDP can be concluded as follows:

Controller ΔP_{ref_1} :

$$K_\infty = \frac{2154.4}{s+63.110} - \frac{12.60}{s+0.301} + \frac{0.20}{s+0.107} \quad (20)$$

Weighting function:

$$W_1 = \frac{50s+5}{s+0.3},\ W_2 = 1 \quad (21)$$

The weighting functions can be selected appropriately by the experienced control engineer. Table I. shows the appropriate values of PID controllers based on GA.

Table 1. Parameters used in the PID controllers.

PID controller	K_P	K_I	K_D
Thermal area	0.5875	-0.0498	-0.1283
Hydro area	-0.4516	-0.0599	0.5281

The frequency response of the hydro-thermal power system with the ECS by H_∞ -LSDP reveals that the magnitude and phase of the signal in the system without the controller has less damping yielding the resonance peak of 10 dB. However, after including the controller, the resonance peak is drastically reduced as Figure 6.

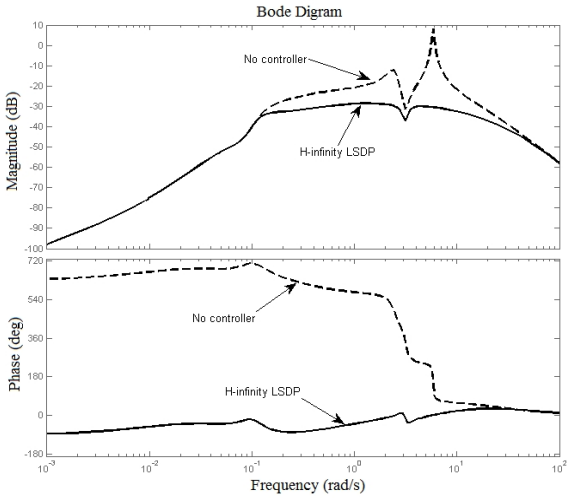

Figure 6. The frequency response of the hydro-thermal power system with the ECS by H_∞ -LSDP.

From the simulation results, the variation of the load by the percentage of 5% of the installed capacity of electricity generation in the

thermal power system make the fluctuation of the generated electrical power in the system. By designing the controller using H_∞ -LSDP, the oscillation is reduced more than when designing PID controller based on GA as in Figure 7-11 accordingly.

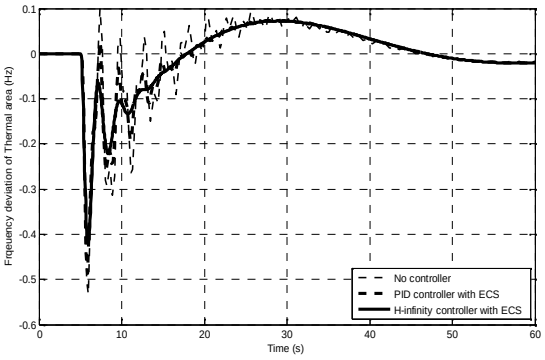

Figure 7. The frequency response of the thermal area (ΔP_{ref_1}) with 5% variation of the load in the thermal area.

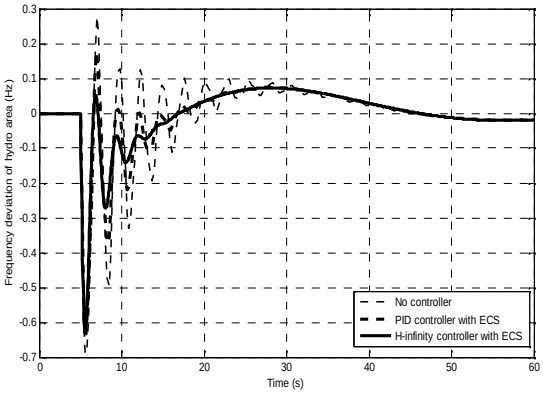

Figure 8. The frequency response of the hydro area (ΔP_{ref_1}) with 5% variation of the load in the thermal area.

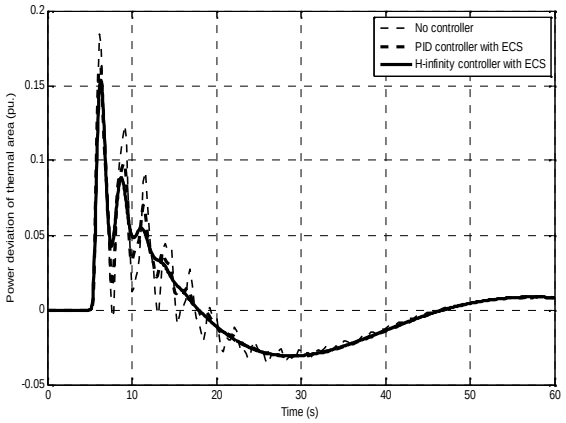

Figure 9. The tie line power response of the hydro area (ΔP_{ref_1}) with 5% variation of the load in the thermal area.

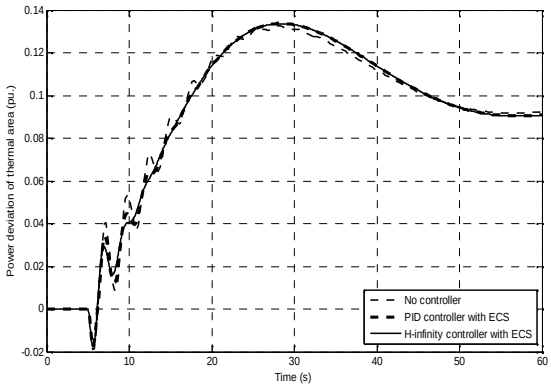

Figure 10. The power response of the thermal area (ΔP_{ref_1}) with 5% variation of the load in the thermal area.

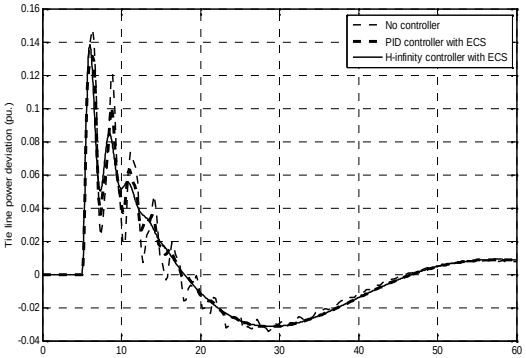

Figure 11. The power response of the hydro area (ΔP_{ref_1}) with 5% variation of the load in the thermal area.

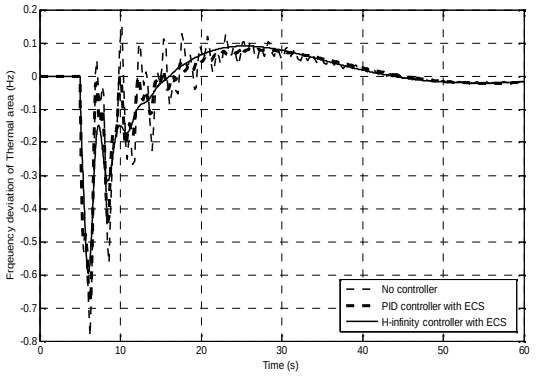

Figure 12. The frequency response of the thermal area (ΔP_{ref_1}) with 10% variation of changing loads in the both of two areas.

In order to demonstrate the robustness of the H_∞-LSDP controller under the changing load at the thermal and hydro area. From Fig. 12-16, when the load at the thermal and hydro area are adjusted such that 10% variation of the load in the both of two areas, the controller designed by H_∞-LSDP can still preserve the stability under the variation of the load in the hydro area better than the PID controller designed by GA.

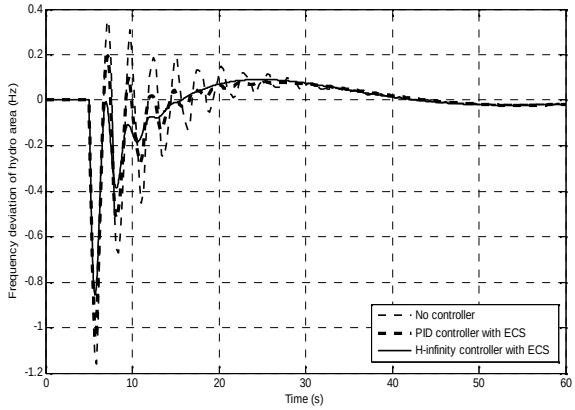

Figure 13. The frequency response of the hydro area (ΔP_{ref_1}) with 10% variation of changing loads in the both of two areas.

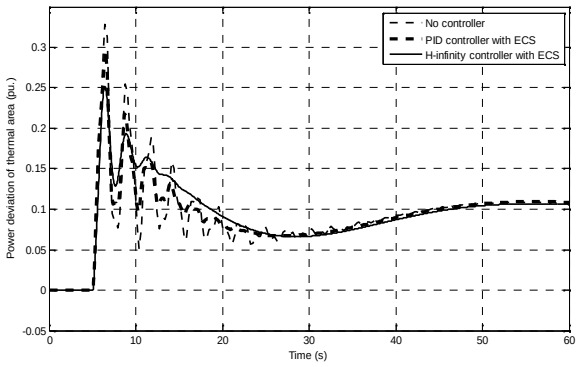

Figure 14. The power response of the tie line (ΔP_{ref_1}) with 10% variation of changing loads in the both of two areas.

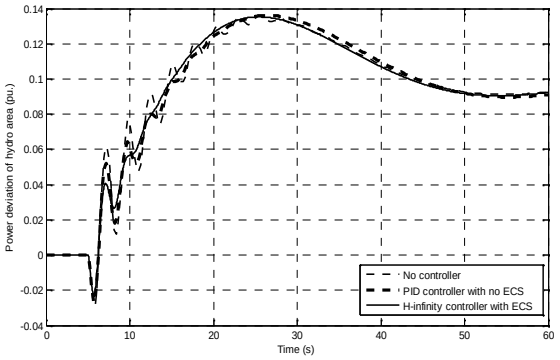

Figure 15. The power response of the thermal area (ΔP_{ref_1}) with 10% variation of changing loads in the both of two areas.

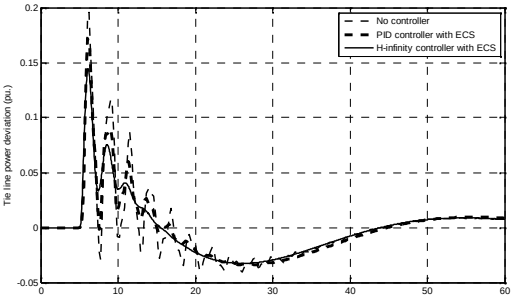

Figure 16. The power response of the hydro area (ΔP_{ref_1}) with 10% variation of changing loads in the both of two areas.

5. CONCLUSION

This paper proposes the robust hydro-thermal power system controller design

methodology considering the ECS in order to improve the stability of the system under the disturbance of the load change in form of 5% variation in the electricity generation. The performance of controllers is compared with the PID controllers tuned by GA. The results are obvious that the PID controllers give poorer stability than the controller designed by H_∞ -LSDP. After the thermal-hydro power system have been adjusted the percentage of 10% of its load, the controller designed by H_∞ -LSDP can still preserve the performance better than the controller designed by GA. Moreover, the efficient usage of the ECS was illustrated and approved.

APPENDIX

A. System Data.

$T_G = 0.08$ s, $T_T = 0.3$ s, $T_1 = 42.5$ s,

$T_2 = 0.515$ s, $T_R = 5$ s, $T_W = 1$ s,

$T = 0.0855$ s, $T_{dc} = 0.05$ s, $T_{P_1} = 20$ s,

$T_{P_2} = 20$ s, $K_{P_1} = 120$ Hz/pu.,

$K_{P_2} = 120$ Hz/pu., $a_{12} = -1$,

$_1 = \ _2 = 0.424$, $R_1 = R_2 = 2.4$ Hz/pu.

B. Energy Capacitor System.

$K_{VD} = 0.1$ KV/KA, $K_0 = 69$ KV/Hz, $C = 1$F,

$R = 100\ \Omega$, $E_{D_0} = 2$ KV.

REFERENCES

[1] Green, R. K., 1996, Transformed automatic generation control, IEEE Trans. Power Systems, vol. 11, pp. 1799-1804,.

[2] Karnavas, Y. L., & D. P. Papadopoulos, 2002, AGC for autonomous power system using combined Intelligent techniques, International Journal of Electrical Pow1er System Research, vol. 62, pp. 225-239.

[3] Tripathy, S. C., M. Kalantar, R. Balasubramanian, 1991, Dynamics and stability of wind and diesel turbine generators with superconducting magnetic energy storage unit on an isolated power system, IEEE Trans. Energy Conversion, vol. 6, pp. 46-51.

[4] Banerjee, S., J. K. Chatterjee, & S. C. Tripathy, 1990, Application of magnetic energy storage unit as load frequency stabilizer, IEEE Trans. Energy Conversion, vol. 5, pp. 46-51,.

[5] Nakata, S., K. Yoshioka, A. Yoshida, & H. Yoneda, 2001, Advanced capacitors and their application, Journal of Power Sources, pp. 97-98,.

[6] Yaser S. Q., A. A. Elbaset, & T. Hiyama, 2011, Simulation studies on ECS application in a clean power distribution system, Electrical Power and Energy Systems 33 , pp. 43–54.

[7] IEEE Committee Report, 1970, Standard definitions of terms for automatic generation control on electrical power systems, IEEE Trans. Electric Power Apparatus System, pp. 89.

[8] IEEE PES Committee Report, 1973, Dynamic models for steam and hydro turbine in power system studies, IEEE Trans. Power Apparatus System, pp. 92.

[9] IEEE PES Working Group, 1992, Hydraulic turbine and turbine control models for system dynamics, IEEE Trans. Power System, pp. 7.

[10] Glover, K., D. Mcfarlane, 1989, Robust stabilization of normalized coprime factor plant description with H_∞ -bounded uncertainty, IEEE Trans. Automatic control, vol. 34, no. 8, pp. 821-830.

[11] Bevrani, H., 2009, Robust Power System Frequency Control, Springer,.
[12] Goldberge, D. E., 1989, Genetic Algorithm in Search, Optimization and Machine Learning, Addison-Wesley publishing Company Inc.
[13] Skogestad, S., & I., 2005, Postlethwaite, Multivariable Feedback Control Analysis and Design, John Wiley.